



# A Geometric Approach to Task-Specific Cartesian Stiffness Shaping

Nikola Knežević<sup>1</sup> · Branko Lukić<sup>1</sup> · Tadej Petrič<sup>2</sup> · Kosta Jovanović<sup>1</sup>

Received: 19 July 2023 / Accepted: 12 December 2023 / Published online: 17 January 2024  
© The Author(s), under exclusive licence to Springer Nature B.V. 2024

## Abstract

Controlling the exact Cartesian stiffness values of a robot end-effector (EE) is troublesome because of difficulties associated with estimating the stiffness and controllability of a full Cartesian stiffness matrix. However, most practical applications require only quantitative (high/low) stiffness values in the EE motion direction (or perpendicular direction). Full control of the stiffness matrix requiring too many control inputs which is hardly possible in practical applications. To ensure the efficiency of execution for a range of redundant robots, we present an algorithm for shaping a robot's Cartesian stiffness ellipsoid, a more intuitive and visual stiffness representation, using a nonlinear sequential least square programming optimization. The algorithm is designed to optimize the joint stiffness values and the trajectory of the robot's joints, using null-space exploration, for a given task. Using eigenvalue decomposition of the stiffness matrix, the algorithm minimizes the orientation difference between the major axis of the current and the desired stiffness ellipsoid and specify a scaling factor between the major and the minor axis. The presented approach allows the user to better understand and control of a robot, regardless of the user's knowledge of the achievable stiffness range and the interdependencies of the Cartesian stiffness matrix elements.

**Keywords** Compliance and impedance control · Collaborative robots · Optimization and optimal control · Physical human-robot interaction

## 1 Introduction

With the development of robotics technologies (cobots, sensors, interfaces), robots have mastered and are deployed to a broader range of tasks. However, for a robot to work in an unstructured environment, it has to be safe for humans, the environment, and itself. To ensure safety of physical human-robot interaction [1] and robustness of in-contact task execution, the robot needs to be compliant. Compliance properties can be expressed with its end-effector (EE)

Cartesian stiffness. The EE Cartesian stiffness can be represented numerically or graphically. Numeric representations are stiffness and compliance matrices, whereas the graphical representation for 3D space is a stiffness ellipsoid.

There are three main approaches to achieve Cartesian compliance of a robot's EE: (i) software-based (active) compliance for a wide range of robots in different realizations with and without an additional Force-Torque (FT) sensor at the EE [2, 3]; (ii) software-based (active) compliance for robots with joint torque sensors [4], and (iii) hardware-based (intrinsic) compliance by robot design usually through novel compliant actuation approaches [5]. Approach (i) is compliance at the EE level, while approaches (ii) and (iii) are at a joint level. Nevertheless, each of the three approaches can exploit the redundancy (null-space) in kinematically redundant tasks to shape the EE Cartesian stiffness matrix, adhering to limitations such as the geometry and configuration of the robot, the degree of task redundancy or the joint stiffness range [6, 7].

Both active compliance approaches (i) and (ii) suffer from the non-zero response time in control of intrinsically stiff robots in a contact scenario, whereas (i) is restricted only to reactions to EE collisions. Passive compliance comprising elasticity (iii) between the actuator and the robot link can

✉ Nikola Knežević  
knezevic@etf.rs

Branko Lukić  
branko@etf.rs

Tadej Petrič  
tadej.petric@ijs.si

Kosta Jovanović  
kostaj@etf.rs

<sup>1</sup> School of Electrical Engineering, University of Belgrade, Bulevar kralja Aleksandra 73, Belgrade 11000, Serbia

<sup>2</sup> Department of Automatics, Biocybernetics, and Robotics, Jožef Stefan Institute, Jamova cesta 39, Ljubljana 1000, Slovenia

enhance safety during impact [8, 9], exploiting the design of serial elastic actuators (SEA) and variable stiffness actuators (VSA). Cartesian stiffness shaping that uses kinematic redundancy can be applied to both active and passive compliance [4, 10, 11].

As analyzed in [10], for a 3D task, at least 14 variable stiffness joints are required to control the EE Cartesian position (6 degrees of freedom (DoFs)) and a full stiffness matrix (21 DoFs). Obviously, this is not feasible for standard robot configurations. Some optimization and prioritization are necessary [12, 13]. A two-part EE Cartesian stiffness control/optimization (fast and slow) of a kinematic redundant VSA-driven robot is proposed in [10]. Fast optimization takes place in the joint stiffness space and slow (non-linear) optimization in the robot's null-space.

In [12], the authors propose an active impedance controller in addition to the modulation of stiffness in joints with passive compliance to enable shaping of the whole Cartesian stiffness matrix. Active impedance control is predominantly exploited to shape non-diagonal stiffness matrix elements. However, the approach still targets the exact shaping of a full Cartesian stiffness matrix, which can be challenging. Nevertheless, the authors of [14] point out that control of the diagonal elements of the stiffness matrix is essential in most applications. For VSA-driven robots, it is possible to extend the redundant inverse kinematics problem to include variable compliance in each joint and obtain compliance extended inverse kinematics [15].

Also, EE Cartesian compliance shaping can be divided into configuration-dependent stiffness (CDC) and common mode stiffness (CMS) [11]. CDC comes from a redundant robot configuration and is used to orientate the stiffness ellipsoid, while CMS affects the ellipsoid volume. CMS represents an additional degree of freedom that can be included in inverse kinematics to obtain better results.

The EE Cartesian stiffness matrix depends on the robot's pose through the Jacobian matrix, as well as on stiffness on a joint level, which represents nonlinear expressions from the joint position and stiffness to EE Cartesian stiffness. Because of this, it is hardly possible for a typical 6-7 DoF robot to find an analytical set of joint positions/stiffness that will satisfy the desired EE position and shape a full stiffness matrix. Therefore, the optimization techniques that exploit null-space are necessary for finding approximate solutions that minimize targeted discrepancies in robot positioning or Cartesian stiffness shaping [13, 16]. In [7], the authors demonstrate the efficiency of the SLSQP approach on a 4-DoF SEA planar robot. However, this was restricted to the shaping of Cartesian stiffness in a static position by matching the exact values of the diagonal elements of the Cartesian stiffness matrix.

Also, considerable research has been done in the field of impedance control to make a robot compliant. Traditionally, impedance control has been based on selecting controller gains that will provide a trade-off between allowable positioning errors and acceptable interaction forces [17]. The selection of appropriate impedance gains is not a trivial task for non-expert users, due to the complexity that arises from a given task or the complexity of the control method itself [18–20]. To overcome unintuitive and complex shaping of gains for impedance controllers, an adaptive and iterative learning approach is adopted to tackle the problem of impedance planning [21, 22]. Recent research [23] addresses the problem of impedance planning for Cartesian impedance controllers that do not assign closed-loop inertia. A task-based impedance shaping algorithm is proposed in [24].

All the above-mentioned approaches find usage in practical applications. In [25], the authors propose the use of impedance control for collaborative human-robot chamfering and polishing applications. Also, null-space search is proposed in [26] for torque-effective drilling. The researchers in [27] introduce collaborative assembly shaping robot behavior with active and passive compliance.

In related literature, Cartesian stiffness shaping for the robot EE mostly focuses on algorithms that exploit kinematic redundancy and/or joint compliance for fitting all components of the Cartesian stiffness matrix [28–30]. However, exact numerical stiffness shaping is impossible in most practical tasks due to challenges associated with stiffness estimation, knowledge about the achievable stiffness range (due to a limited joint stiffness range and dependence on the robot's pose), and formulating quantitative indicators of the desired stiffness. Furthermore, stiffness planning through fitting of the Cartesian stiffness matrix is especially demanding in trajectory-dependent tasks.

This paper presents an optimization method for shaping EE Cartesian stiffness along the axes that are essential for predefined tasks and robot EE trajectories. Customizing the design of an objective function, the algorithm can shape the geometrical stiffness representation by setting the ratio between the major and minor axes of the stiffness ellipsoid, which can be used for task-specific targeted behavior (assembling, inserting, pulling through, cutting, drilling, etc.). The desired robot behavior is extracted directly from a trajectory that the robot needs to follow, resulting automatically in an indirect adjustment of the parameters of the Cartesian stiffness matrix. Therefore, the presented approach enables users to better understand and command the robot's Cartesian stiffness regardless of user knowledge about the achievable stiffness range and mutual dependencies of exact values of the Cartesian stiffness matrix. In comparison to general algorithms for controlling the EE Cartesian stiffness,

the proposed method for geometrical EE Cartesian stiffness shaping (GCSS) offers the following advantages:

- additional expensive force/torque sensors are not required;
- the approach relies on kinematic reconfiguration and passive compliance, which does not influence the stability guaranteed with low-level controllers;
- stiffness estimation is not needed for successful in-contact task execution;
- the method is applicable to any robotic system because it uses common optimization techniques; and
- expert knowledge is not required because shaping is extracted automatically from a given task trajectory.

Additionally, the presented algorithm will contribute to a wider use of collaborative robots, enabling them to perform tasks more efficiently under uncertainty and imperfection of positioning parts that need to be processed, or when faced with disturbance during task execution.

## 2 Methodology

The performance of a task often depends on exerting force on a surface (assembly, polishing, sanding), avoiding high perpendicular contact forces (inserting) and any deviation in the direction of movement (cutting, drilling). For such tasks, it is desirable that the contact force vector is aligned with one of the axes essential for task execution. Generally, to successfully perform arbitrary contact tasks, a robot should be able to fully shape its EE Cartesian stiffness. However, shaping of the full Cartesian stiffness matrix is not applicable in most cases since it requires setting of 21 parameters in total [10].

Nevertheless, Cartesian stiffness shaping can be achieved to some extent with regard to available controllable inputs. Mutual independence of different stiffness terms that shape the stiffness matrix can be represented geometrically in 3D space as a stiffness ellipsoid to provide an intuitive representation to the user. For example, a cutting task requires force to be applied to the cutting surface, with no restrictions or specific requirements for perpendicular tool motion. Therefore, the speed and quality of task execution depend on the stiffness a robot (and tool) is able to produce in the direction of cutting, parallel to the surface to be cut. Knowing that the stiffness ellipsoid volume does not change significantly for specific compliance in joints, kinematic redundancy should be exploited to enlarge and direct the main axis of the stiffness ellipsoid to be parallel to the surface. By contrast, for tasks that require precise trajectory tracking regardless of possible disturbances (e.g., pulling a ring along a wire [31]), the highest stiffness is required in the perpendicular plane to restrict deviation from the trajectory. To that end, the stiffness ellipse

should be shaped to align its longest axis with the plane perpendicular to the trajectory during motion.

To successfully perform the largest number of contact tasks with a given robot, one needs to design an appropriate EE trajectory and shape EE Cartesian stiffness to perform a desired interaction or deal with unexpected disturbances and uncertainties. By applying the methodology presented in this paper, even unskilled workers can successfully provide the robot with optimal joint positions to execute complex tasks while satisfying task specifications. Figure 1 shows the GCSS algorithm flow from the task-specific trajectory towards the optimal joint positions, which will ensure proper task execution with regard to robot kinematics, constraints, and the initial joint stiffness setting. The user needs to provide the desired task-specific EE trajectory and the desired scaling factor between the ellipsoid axes, which refer to the shape of the stiffness ellipsoid and its direction. Processing over a trajectory is necessary to find the optimal joint configuration. The optimization algorithm uses the EE trajectory as a constraint to ensure that the EE will follow that exact trajectory. The desired orientation of the major axis of the EE Cartesian stiffness ellipsoid is also computed from the EE trajectory. Based on task-specific motion, a proper joint stiffness set is computed to initially orient the major axis of the EE Cartesian stiffness ellipsoid in the motion direction, where these values are used as constant parameters for the optimization algorithm. Finally, the optimization algorithm provides task-optimal joint configurations from the kinematic model of the robot, the initial joint stiffness setting, and the desired orientation of the major axis of the ellipsoid.

### 2.1 Cartesian Stiffness Modeling and Geometrical Representation

This paper presents an optimization algorithm for shaping the stiffness ellipsoid in the direction of movement of a robot's EE. The algorithm exploits null-space to find the optimal robot configuration in a certain Cartesian position to achieve the desired stiffness ellipsoid orientation of the major axis as far as possible. The proposed GCSS approach considers the Cartesian robot position and the available joint motion range as constraints, whereas the joint stiffness and Cartesian stiffness ellipsoid parameters are passed to the optimization algorithm as constant parameters. To that end, it is essential to recall the relations between joint stiffness and Cartesian stiffness, as well as the geometrical representation of the Cartesian stiffness matrix. If

$$\mathbf{K}_j = \begin{bmatrix} k_{j1} & 0 & \dots & 0 \\ 0 & k_{j2} & \dots & 0 \\ \vdots & \vdots & \ddots & \vdots \\ 0 & 0 & \dots & k_{jn} \end{bmatrix}, \quad (1)$$

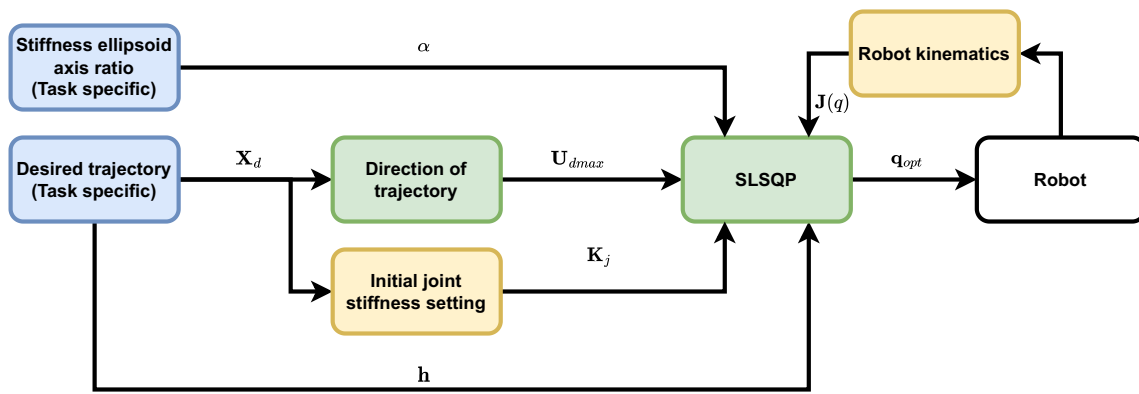


**Fig. 1** Block diagram of the algorithm. Blue blocks represent task-specific inputs, green blocks the main components of the algorithm, and yellow blocks the optimization parameters

is the joint stiffness matrix, where  $k_{ji}$  is the  $i$ -th joint stiffness, and  $J$  is the robot's EE Jacobian matrix, then the Cartesian stiffness matrix can be computed as follows:

$$K_C = (J(q)K_j^{-1}J(q)^T)^{-1}, \tag{2}$$

where  $q$  is the joint position vector. Using eigen-decomposition, the Cartesian stiffness matrix can be decomposed and represented in the form

$$K_C = U\Lambda U^{-1}, \tag{3}$$

where  $U$  is the matrix of eigenvectors and  $\Lambda$  is the matrix with eigenvalues that can be extracted from eigen-decomposition of the EE Cartesian stiffness square matrix. The matrix  $U = [U_1, U_2, \dots, U_n]$  is composed of eigenvectors  $U_i = [u_{i1}, u_{i2}, \dots, u_{in}]^T$  for  $i = 1 \dots n$ , and matrix  $\Lambda$  is a diagonal matrix composed of eigenvalues

$$\Lambda = \begin{bmatrix} \lambda_1 & 0 & \dots & 0 \\ 0 & \lambda_2 & \dots & 0 \\ \vdots & \vdots & \ddots & \vdots \\ 0 & 0 & \dots & \lambda_n \end{bmatrix}. \tag{4}$$

The Cartesian stiffness matrix can be represented geometrically as an ellipsoid, where the columns of matrix  $U$  represent unit vectors of an ellipsoid axis, while the diagonal elements of matrix  $\Lambda$  represent axis magnitudes. The orientation of the stiffness ellipsoid is defined by the major ellipsoid axis. After eigen-decomposition, the ellipsoid parameters can be calculated as

$$\lambda_{\max} = \max_{i \in [1, n]} (\lambda_i), \tag{5}$$

$$\lambda_{\min} = \min_{i \in [1, n]} (\lambda_i), \tag{6}$$

where  $\lambda_{\max}$  is the magnitude of the major stiffness ellipsoid axis and  $\lambda_{\min}$  is the minor stiffness ellipsoid axis. The

stiffness ellipsoid direction vector is represented by  $U_{\max}$ , which is an eigenvector from  $U$  that corresponds to the largest eigenvalue from  $\Lambda$  (orientation of the major stiffness ellipsoid axis). Using the geometrical representation of the Cartesian stiffness matrix, the user can more intuitively monitor and command the desired Cartesian stiffness properties of the robot's EE.

### 2.2 SLSQP as an Optimization Approach for EE Cartesian Stiffness Shaping

Cartesian stiffness shaping of robots with joint compliance (real or software-emulated) is commonly approached through robot reconfiguration in null-space for kinematically redundant tasks [3, 4, 13] or through joint stiffness modulation for VSA-driven robots [12]. The non-linear optimization algorithm based on the sequential least square programming (SLSQP) approach is used to find task-optimal robot properties, such as joint stiffness and robot configuration [7]. The SLSQP approach is implemented due to its efficiency demonstrated in high-dimensional non-linear problems [32, 33]. Consequently, its effectiveness has been extensively demonstrated in the context of trajectory and robot configuration optimization within the field of robotics [34, 35]. The problem statement can be formulated as follows:

$$\begin{aligned} \min f(q), \text{ over } q \in \mathbb{R}^n, \\ \text{subject to } h(q) = 0, \\ g(q) \leq 0, \end{aligned} \tag{7}$$

where the objective function is represented as  $f : \mathbb{R}^n \rightarrow \mathbb{R}$ , while functions  $h : \mathbb{R}^n \rightarrow \mathbb{R}^m$  and  $g : \mathbb{R}^n \rightarrow \mathbb{R}^z$  represent equality and inequality constraints for an optimization problem. The value  $n$  represents the number of variables in vector  $q$  (robot's joints position vector) for which optimization is performed, and  $m$  and  $z$  are the number of equality or inequality constraints, respectively.

The algorithm transforms the non-linear objective function  $f(\mathbf{q})$  to a quadratic function in each iteration  $\mathbf{q}[k]$ , trying to solve the problem using the quadratic programming approach. The algorithm uses the  $k^{\text{th}}$  iteration output -  $\mathbf{q}[k]$  as input for the next iteration  $\mathbf{q}[k + 1]$ . These steps are repeated until  $\mathbf{q}[k]$  converges to the local minimum  $f(\mathbf{q}^*)$  of the optimization problem Eq. 7 while satisfying all constraints, where  $*$  represents the local minimum point.

The criterion function  $f$  is designed to minimize the difference  $\theta$  between the orientation of the major axis of the desired Cartesian stiffness ellipsoid and the current Cartesian stiffness ellipsoid. Since vectors  $\mathbf{U}_{c \max}$  and  $\mathbf{U}_{d \max}$  are unit vectors the angle between them can be found as:

$$\theta = \arcsin(|\mathbf{U}_{c \max} \times \mathbf{U}_{d \max}|), \quad (8)$$

where  $\mathbf{U}_{c \max}$  is the major axis direction vector of the current stiffness ellipsoid,  $\mathbf{U}_{d \max}$  is the major axis direction vector of the desired stiffness ellipsoid, which follows from geometrical representation of vector product.

Based on task-specific requirements, the desired stiffness ellipsoid orientation can be set along or perpendicular to the trajectory. In cases where the major axis of the desired stiffness ellipsoid is oriented along the trajectory, the criterion function  $f$  is defined as follows:

$$f = \frac{|\theta|}{\beta}, \quad (9)$$

or if the orientation of the major axis of the desired stiffness ellipsoid is perpendicular to the trajectory

$$f = \frac{\frac{\pi}{2} - |\theta|}{\beta}, \quad (10)$$

where  $\theta$  is angle between desired and current stiffness ellipsoid and  $\beta$  is the scaling factor that ensures that the stiffness ellipsoid axes satisfy the desired ratio.

The scaling ratio  $\beta$  is defined as follows:

$$\beta = \min\left(\frac{\lambda_{\max}}{\lambda_{\min}}, \alpha\right), \quad (11)$$

where  $\alpha$  is the maximal ratio that the stiffness ellipsoid axes need to achieve. Scaling factor  $\beta$  is incorporated directly in the criteria function  $f$  and, consequently, the optimization result will combine the effect of stiffness ellipsoid orientation and ellipsoid axis ratio. The equality constraints represent the difference between the current and desired EE positions, which should be 0, to ensure trajectory tracking

$$\mathbf{h}(\mathbf{q}) = \mathbf{X}_c(\mathbf{q}) - \mathbf{X}_d = 0, \quad (12)$$

where Cartesian coordinates with the index  $c$  represent the robot EE position and orientation based on optimization variable  $\mathbf{q}$ , whereas Cartesian coordinates with the index  $d$  are the desired robot EE position and orientation. In addition, appropriate lower and upper bounds must be set to ensure that the optimization search does not go beyond the available joint motion range, which is dictated by the geometric parameters of the robot.

By applying the procedure described above, the orientation of the major axis of the desired EE Cartesian stiffness ellipsoid and the axis ratio can be set to ensure proper robot behavior for various tasks.

### 2.3 Initial Joint Stiffness Setting

Initial search is undertaken to find the initial joint stiffness for a specific task. Three points are selected on the EE trajectory: first, middle, and last. The optimization algorithm Eq. 7 is executed and joint stiffnesses are optimization variables. The value of the criteria function used to find initial joint stiffness  $f_{ijs}$  is calculated as follows:

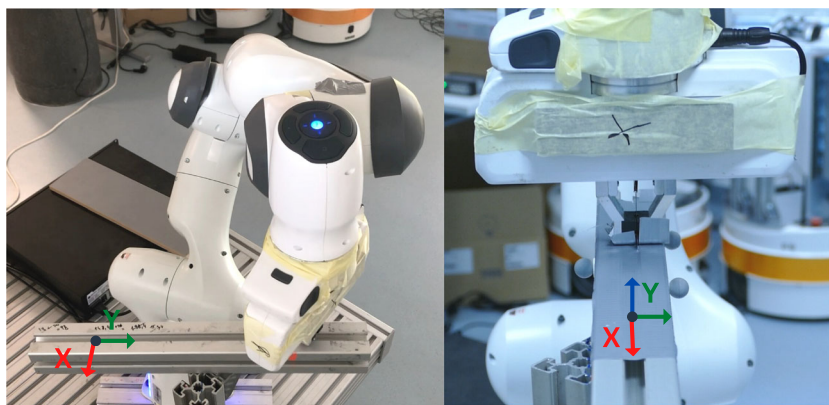
$$f_{ijs} = [f(\text{first}) + f(\text{middle}) + f(\text{last})], \quad (13)$$

where  $f$  represents the criteria function defined in Eqs. 9 or 10, depending on task requirements. In this way, the calculated joint stiffness values enable the EE Cartesian stiffness ellipsoid to align with the trajectory, as much as possible.

## 3 Experimental Evaluation

The 7DoF Panda robot [36] with software-based adjustable joint stiffness was used for experimental evaluation. The robot performed a motion that was calculated offline as a result of the optimization algorithm. For the optimization *MATLAB R2021a fmincon* tool was used, with *active-set* solver with constraint tolerance and function tolerance  $1e^{-5}$  and  $1e^{-2}$ , respectively. The time taken to optimize the robot's movement along the entire path was  $0.4 \pm 0.1$  s. Two different tasks were carried out. The first task was pulling a bolt through an aluminum profile, as shown in Fig. 2 (left). The second task was tape cutting (Fig. 2, right). Selected tasks require similar robot behaviors like a peg-in-hole, object insertion, polishing, drilling, and screwing, where the EE Cartesian stiffness ellipsoid needs to be oriented along the robot trajectory or perpendicular to it. First, the GCSS algorithm and its properties were evaluated in a simulation environment. Then, the task-optimal joint configuration was implemented on the real robot. There were four experiments for the first task and two for the second task. Without losing generality, both tasks were planar. In that case, the

**Fig. 2** Pulling bolt through aluminum profile experiment (left) and tape cutting experiment (right)



2D Cartesian stiffness ellipse could be used instead of the ellipsoid. A demonstration of both tasks in all the experiments is provided on the following link <https://youtu.be/ApsIJwaJIbo>.

### 3.1 Simulation Algorithm Evaluation

The task of pulling a bolt through an aluminum profile was selected to showcase algorithm properties in the MuJoCo simulation environment [37]. An inverse kinematic controller drove the robot through referent trajectories without consideration of stiffness properties to illustrate basic robot behavior. The task-specific orientation of the major axis of the EE Cartesian stiffness ellipse was extracted from the reference trajectory, where the trajectory direction represented the desired orientation of the major axis of the EE Cartesian stiffness ellipse.

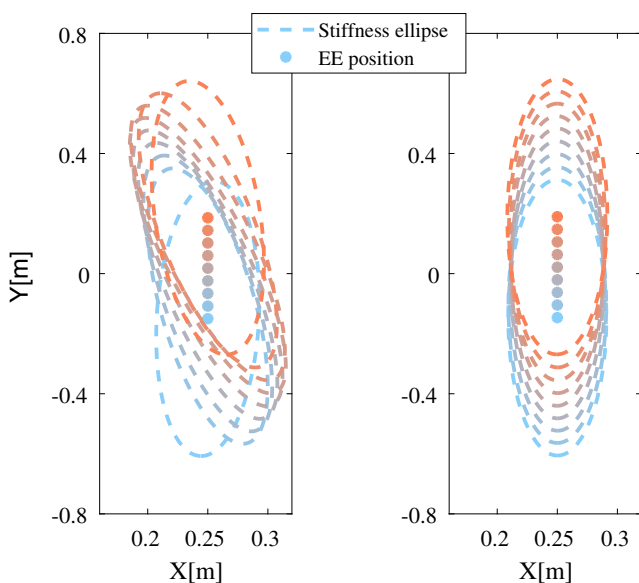


**Fig. 3** End-effector stiffness ellipse orientation along the motion direction (from blue to red dot), non-optimal scenario (left), and optimal scenario (right)

The task-specific joint stiffness matrix was calculated according to Eq. 13 from Section 2.3 and set to  $\mathbf{K}_j = \text{diag}(1200, 20, 1200, 20, 250, 20, 20) \frac{\text{Nm}}{\text{rad}}$ . Based on an inverse kinematic controller, the robot achieves a joint configuration that is, in the general case, not optimal for a specific task in terms of expected or non-intended interactions. The stiffness ellipse for the desired Cartesian trajectory prior to Cartesian stiffness shaping is shown in Fig. 3 left. The GCSS algorithm found the optimal robot configuration to satisfy all constraints (EE desired trajectory and available joint motion range) and orient the major axis of the EE Cartesian stiffness ellipse in the desired direction, as presented in Fig. 3 right.

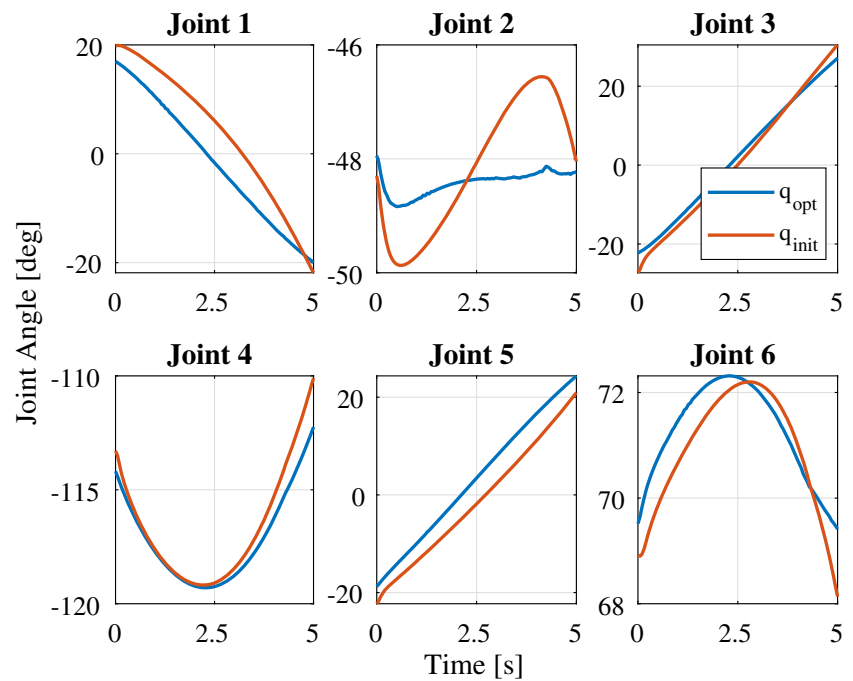
The joint trajectories in the non-optimal and optimal scenarios are depicted in Fig. 4, where the 7<sup>th</sup> joint does not appear because the task was 5DoF and the 7<sup>th</sup> joint did not influence task execution (rotation about Z-axis). In both scenarios, non-optimal and optimal, robot motion started from an identical configuration. The effect of null-space reconfiguration during desired trajectory tracking presented in Fig. 4 confirms the success of the GCSS algorithm, satisfying the constraints while aligning the EE Cartesian stiffness ellipse along the direction of motion (Fig. 3). The error in the orientation of the major axis of the EE Cartesian stiffness ellipse over the whole trajectory was less than 0.1 degrees.

### 3.2 The Task of Pulling a Bolt Through an Aluminum Profile

To complete the bolt pulling task, the major axis of the robot's EE Cartesian stiffness ellipse needed to be oriented along the aluminum profile. This means that the major axis of the stiffness ellipse had to be oriented along the robot's direction of movement, while allowing lateral motion in order to avoid high interaction forces and friction.

In several studies, authors have undertaken comparisons between their Cartesian stiffness modulation algorithms and naive-base control approaches to highlight the advantages of their methods [23, 38, 39]. In this paper, four different experiments were conducted, showcasing the differences between

**Fig. 4** Joint positions resulting from embedded inverse kinematic controller (red) and stiffness shaping optimization controller (blue)



the GCSS algorithm and the naive-base approach control methods. In the first experiment (Fig. 5a), the robot was controlled by the GCSS algorithm to pull the bolt through the aluminum profile with no disturbance to the environment. In the second experiment (Fig. 5b), the stiffness of all robot joints was low, making the robot compliant. In the third experiment (Fig. 5c), the stiffness of all robot joints was high (the robot was stiff). For the second, third, and fourth experiments, the aluminum profile was rotated about its end, effectively applying disturbance to the task. The proposed GCSS algorithm controlled the robot in the fourth experiment (Fig. 5d). It is apparent that the robot executed the task successfully when there were no disturbances (Fig. 5a). There were no errors in tracking the commanded trajectory. Also, the algorithm was successful in orienting the main axis of the EE Cartesian stiffness ellipse along the direction of movement. At  $t = 4$  s, the robot exited the aluminum profile, continued to move in free space, and external forces dropped down to zero.

In the experiment executed in the compliant mode (Fig. 5b), the robot was unable to accomplish the given task in the presence of a disturbance. The orientation of the main axis of the EE Cartesian stiffness ellipse in this experiment was not optimal. Therefore, due to the low Cartesian stiffness, the bolt got stuck under the influence of the disturbance and interaction force for  $t = 5$  s. At that point, the robot's accumulated energy was high enough to release the robot. It continued to move, but did not succeed in finishing the task. The robot also failed to complete the task in the stiff mode (Fig. 5c). At  $t = 1$  s, the external forces that acted on the EE exceeded the collision threshold, causing the robot to stop

moving. In the final experiment (Fig. 5d), the robot used the GCSS algorithm and accomplishes the task. The orientation of the major axis of the robot's EE Cartesian stiffness ellipse remained unchanged and optimal during the entire execution. Because of the optimal orientation and shaping of the Cartesian stiffness ellipse, the robot was able to adapt to the applied disturbance (deviation in the  $X$  direction) and successfully track the position in the  $Y$  direction. At  $t = 4$  s, the robot exited the aluminum profile and this decreased external forces to zero and also decreased the position error in the  $X$  direction.

### 3.3 The Cutting Task

In the first tape cutting experiment, the desired orientation of the major axis of the EE Cartesian stiffness ellipse was set along the direction of cutting, while in the second experiment it was perpendicular. The orientations of the major axis of the EE Cartesian stiffness ellipse in these two experiments after the GCSS algorithm are illustrated in Fig. 6. It is apparent that in both experiments the GCSS algorithm was capable of achieving the desired orientation of the major axis of the EE Cartesian stiffness ellipse.

While performing the cutting task, the robot needed to apply a force of approximately 10 N in the direction of cutting to penetrate the tape successfully (see Fig. 7 (top)). In the first experiment (highlighted in blue), the robot achieved the cutting force faster because, in that case, the robot's EE Cartesian stiffness was higher in the direction of cutting. Thus, any deviation from the reference trajectory was minimal and the robot accomplished the tape cutting task (Fig. 7 (bottom)).

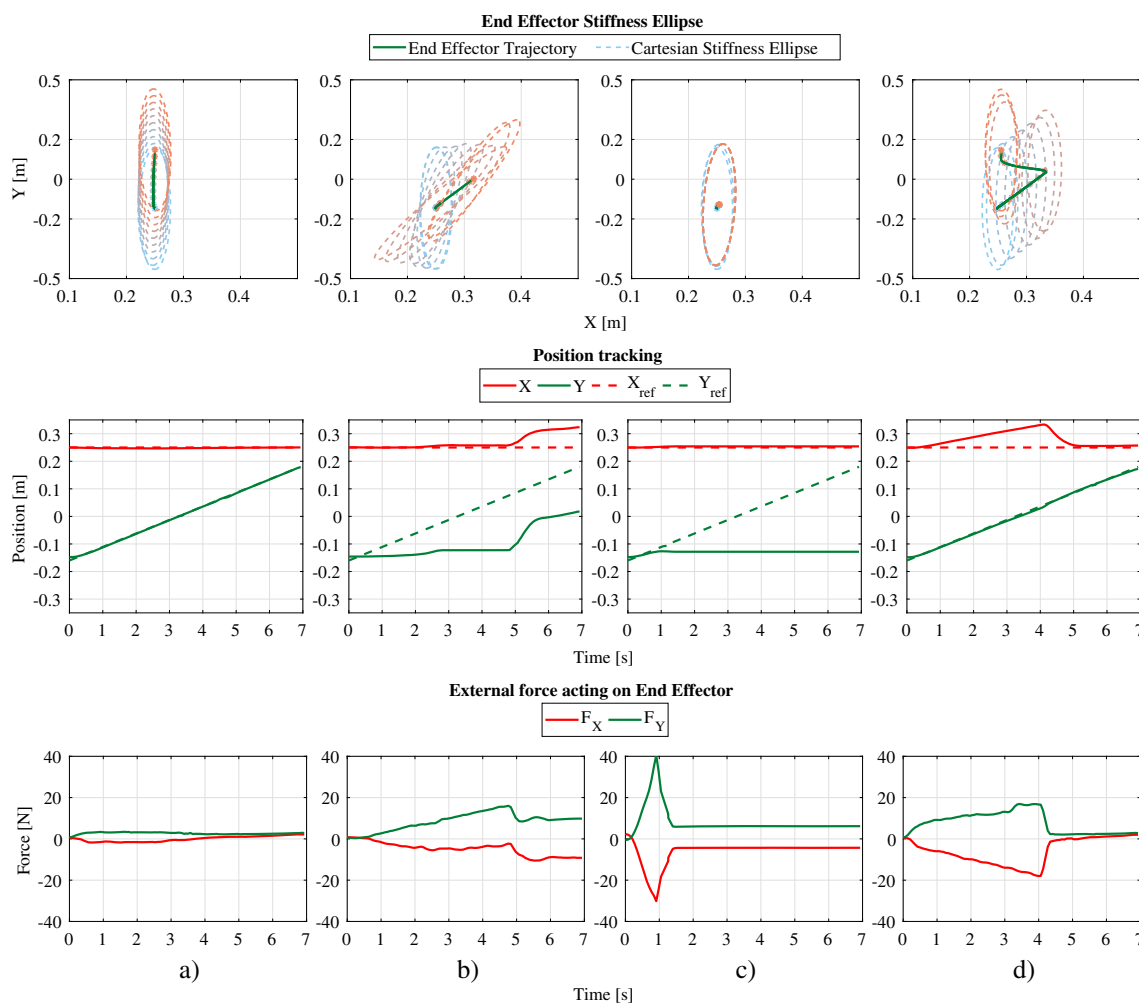


**Fig. 5** Pulling bolt through aluminum profile experiment. a) GCSS algorithm mode without disturbance; b) Compliant mode with disturbance; c) Stiff mode with disturbance; and d) GCSS algorithm with disturbance

In the second experiment (highlighted in orange), where the major axis of the robot’s EE Cartesian stiffness ellipse was oriented perpendicular to the direction of cutting, the force required to execute the task was achieved later. The deviation from the reference position was significant in the second case. The position error decreased when the robot achieved the required cutting force. Although the robot reached the appropriate cutting force, the accumulated error was too large and could not be compensated because of the low EE Cartesian stiffness along the direction of cutting, so the cutting process failed (Fig. 7 (bottom)).

### 4 Conclusion

The paper presented a Cartesian stiffness shaping method that overcomes typical challenges in Cartesian stiffness control, such as stiffness estimation, knowledge about the achievable stiffness range, formulation of quantitative indicators in the

Cartesian stiffness matrix, and the requirement to use a force/torque sensor. The proposed approach exploits the geometrical representation of EE Cartesian stiffness and introduces an optimization method for shaping EE Cartesian stiffness along axes that are essential for predefined tasks and commanded robot trajectories. As such, it contributes to user-friendly command of stiffness shaping and task-specific targeted behavior for typical robot tasks (assembly, inserting, pulling through, cutting, drilling, etc.). The optimization method for EE Cartesian stiffness shaping relies on sequential least square programming (SLSQP) to ensure computational efficiency in a non-linear optimization task. The proposed algorithm exploits the kinematic reconfiguration of the robot in null space and utilizes general optimization techniques. Therefore, the presented methodology is general and applicable to different robotic systems. Additionally, the presented algorithm provides a more intuitive approach to performing robot tasks with improved efficiency and reliability under uncertainty or when faced

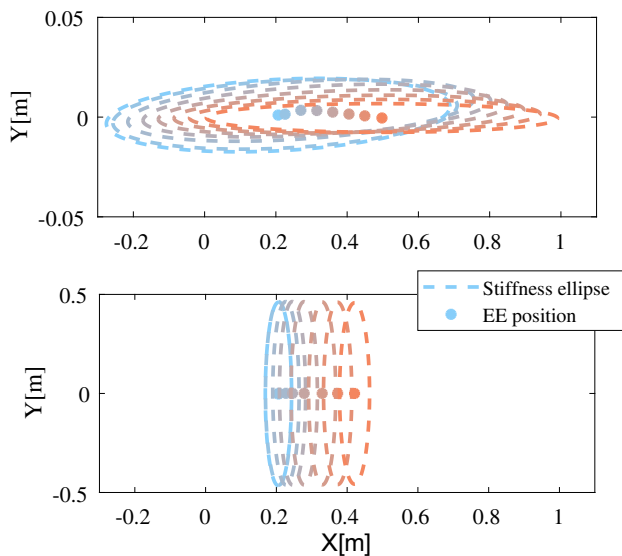


**Fig. 6** End-effector stiffness ellipse orientation for cutting task. Orientation of the major axis of the EE Cartesian stiffness ellipse: Top - along the direction of cutting; Bottom - perpendicular to the direction of cutting

with disturbance during task execution. The algorithm properties and the main benefits of the proposed approach are experimentally demonstrated with two representative in-contact tasks - pulling a bolt through an aluminum profile and cutting. The proposed methodology can be applied to a broad range of tasks in which performance depends on mechanical interaction between a robot and its surroundings.

The limitations of the proposed approach are reflected in two aspects. The first aspect is that in this work, EE Cartesian stiffness is achieved by exploiting passive stiffness. Cartesian

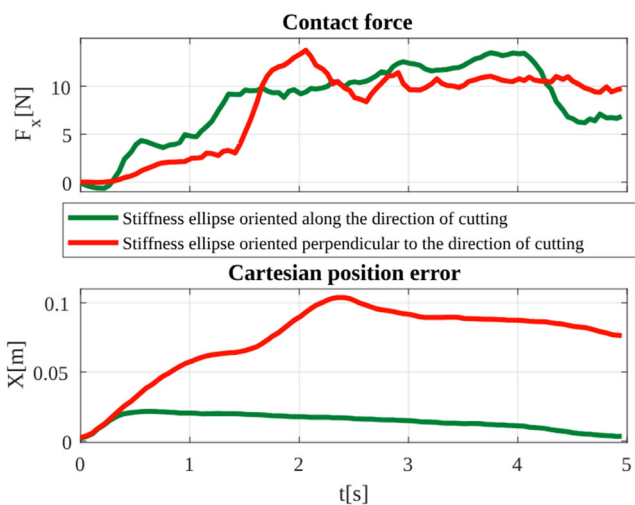


**Fig. 7** End-effector forces in cutting task. Desired EE Cartesian stiffness ellipse oriented along direction of cutting (green). Desired EE Cartesian stiffness ellipse oriented perpendicular to direction of cutting (red)

stiffness is limited due to constraints in the joint stiffness of the robot. The second aspect is that shaping and orienting the stiffness ellipsoid is performed through the exploitation of null-space (kinematic reconfiguration). Due to the manipulator's kinematics, it is sometimes impossible to achieve the desired stiffness ranges when using passive stiffness. In future work, the main focus will be on algorithms that combine active and passive stiffness control at the joint level to enhance the algorithm's performance.

**Supplementary Information** The online version contains supplementary material available at <https://doi.org/10.1007/s10846-023-02035-6>.

**Acknowledgements** This research was supported by the Science Fund of the Republic Serbia, #6784, Modular and versatile collaborative intelligent waste management robotic system for circular economy - CircuBot and Slovenian Research Agency grant N2-0269.

**Author Contributions** All authors contributed to the study conception and design. Conceptualisation, resources and funding acquisition were done by Kosta Jovanović and Tadej Petrič. Material preparation, data collection and analysis were performed by Nikola Knežević and Branko Lukić. The first draft of the manuscript was written by Nikola Knezevic and all authors commented on previous versions of the manuscript. All authors read and approved the final manuscript.

**Funding** This research was supported by the Science Fund of the Republic Serbia, #6784, CircuBot and Slovenian Research Agency grant N2-0269.

**Availability of data and materials** Not applicable

**Code availability** Not applicable

## Declarations

**Ethics approval** Not applicable

**Consent to participate** Not applicable

**Consent to publication** Not applicable

**Competing interests** The authors declare that they have no competing interests that could have influenced the research, analysis, or interpretation of the data presented in this manuscript.

## References

1. Santis, A.D., Siciliano, B., Luca, A.D., Bicchi, A.: An atlas of physical human-robot interaction. *Mech. Mach. Theory* **43**, 253–270 (2008)
2. Hogan, N.: Impedance control: an approach to manipulation: Part ii-implementation. *J. of Dynamic Systems, Measurement, and Control* **107**, 8–16 (1985)
3. Ficuciello, F., Romano, A., Villani, L., Siciliano, B.: Cartesian impedance control of redundant manipulators for human-robot co-manipulation. 2014 IEEE/RSJ Int. Conf. on Intelligent Robots and Systems (2014)

4. Ajoudani, A., Tsagarakis, N. G., Bicchi, A.: On the role of robot configuration in cartesian stiffness control 2015 IEEE Int. Conf. on Robotics and Automation (ICRA) (2015)
5. Braun, D.J., et al.: Robots driven by compliant actuators: optimal control under actuation constraints. *IEEE Trans. Rob.* **29**, 1085–1101 (2013)
6. Lukić, B., Jovanović, K., Knežević, N., Žlajpah, L., Petrič, T.: Maximizing the end-effector cartesian stiffness range for kinematic redundant robot with compliance. *Advances in Service and Industrial Robotics* (2020)
7. Knezevic, N., Lukic, B., Jovanovic, K., Zlajpah, L., Petric, T.: End-effector cartesian stiffness shaping - sequential least squares programming approach. *Serbian J. Electric. Eng.* **18**, 1–14 (2021)
8. Ham, R.V., Sugar, T.G., Vanderborght, B., Hollander, K., Lefeber, D.: Compliant actuator designs. *IEEE Robotics Automation Magazine* **16**, 81–94 (2009)
9. Grioli, G., et al.: Variable stiffness actuators: the user's point of view. *The Intern. J. Robotics Res.* **34**, 727–743 (2015)
10. Albu-Schaffer, A., Fischer, M., Schreiber, G., Schoeppe, F., Hirzinger, G.: Soft robotics: what cartesian stiffness can obtain with passively compliant, uncoupled joints?. 2004 IEEE/RSJ Int. Conf. on Intelligent Robots and Systems (IROS) (2004)
11. Ajoudani, A., Gabbicini, M., Tsagarakis, N., Albu-Schäffer, A., Bicchi, A.: Teleimpedance: exploring the role of common-mode and configuration-dependant stiffness. 2012 12th IEEE-RAS Int. Conf. on Humanoid Robots (Humanoids 2012) (2012)
12. Petit, F., Albu-Schäffer, A.: Cartesian impedance control for a variable stiffness robot arm. 2011 IEEE/RSJ Int. Conf. on Intelligent Robots and Systems (2011)
13. Lukić, B., Jovanović, K., Žlajpah, L., Petrič, T.: Online cartesian compliance shaping of redundant robots in assembly tasks. *Machines* **11** (2023)
14. Ang, M., Andeen, G.: Specifying and achieving passive compliance based on manipulator structure. *IEEE Trans. Robot. Autom.* **11**, 504–515 (1995)
15. Rice, J. J., Schimmels, J. M.: Passive compliance control of redundant serial manipulators. *J. of Mechanisms and Robotics* **10** (2018)
16. Lukic, N., Petrovic, P.B.: Complementary projector for null-space stiffness control or redundant assembly robot arm. *Assem. Autom.* **39**, 696–714 (2019)
17. Hogan, N.: Impedance control of industrial robots. *Robotics Computer-Integrated Manufact.* **1**, 97–113 (1984)
18. Neville, H.: Impedance control: an approach to manipulation: Part iii-applications. *J. Dynamic Syst. Measurement Control* **107**, 17–24 (1985)
19. Abu-Dakka, F. J., Saveriano, M.: Variable impedance control and learning—a review. *Frontiers in Robotics and AI* **7** (2020)
20. Martín-Martín, R. et al.: Variable impedance control in end-effector space. an action space for reinforcement learning in contact rich tasks. Proceedings of the Int. Conf. of Intelligent Robots and Systems (IROS) (2019)
21. Yang, B.-H., Asada, H.: Progressive learning and its application to robot impedance learning. *IEEE Trans. Neural Netw.* **7**, 941–952 (1996)
22. Yamawaki, T., Ishikawa, H., Yashima, M.: Iterative learning of variable impedance control for human-robot cooperation. 2016 IEEE/RSJ Int. Conf. on Intelligent Robots and Systems (IROS) (2016)
23. Pollayil, M. J. et al.: Choosing stiffness and damping for optimal impedance planning. *IEEE Transactions on Robotics* 1–20 (2022)
24. Lachner, J., Allmendinger, F., Stramigioli, S., Hogan, N.: Shaping impedances to comply with constrained task dynamics. *IEEE Trans. Rob.* **38**, 2750–2767 (2022)
25. Kana, S., Lakshminarayanan, S., Mohan, D.M., Campolo, D.: Impedance controlled human-robot collaborative tooling for edge chamfering and polishing applications. *Robotics Computer-Integrated Manufact.* **72**, 102199 (2021)
26. Zanchettin, A. M., Rocco, P., Robertsson, A., Johansson, R.: Exploiting task redundancy in industrial manipulators during drilling operations. 2011 IEEE Int. Conf. on Robotics and Automation (2011)
27. Cherubini, A., Passama, R., Crosnier, A., Lasnier, A., Fraise, P.: Collaborative manufacturing with physical human-robot interaction. *Robotics and Computer-Integrated Manufacturing* **40**, 1–13 (2016)
28. Khatib, O.: A unified approach for motion and force control of robot manipulators: the operational space formulation. *IEEE J. on Robotics Automation* **3**, 43–53 (1987)
29. Nakamura, Y., Hanafusa, H., Yoshikawa, T.: Task-priority based redundancy control of robot manipulators. *The Int. J. of Robotics Research* **6**, 3–15 (1987)
30. Siciliano, B., Slotine, J.-J.: A general framework for managing multiple tasks in highly redundant robotic systems. Fifth Int. Conf. on Advanced Robotics 'Robots in Unstructured Environments (1991)
31. Žlajpah, L., Petrič, T.: Unified virtual guides framework for path tracking tasks. *Robotica* **38**, 1807–1823 (2020)
32. Kraft, D.: A software package for sequential quadratic programming Deutsche Forschungs- und Versuchsanstalt für Luft- und Raumfahrt Köln: Forschungsbericht (Wiss. Berichtswesen d. DFVLR, 1988) (1988)
33. Boggs, P.T., Tolle, J.W.: Sequential quadratic programming for large-scale nonlinear optimization. *J. Comput. Applied Math.* **124**, 123–137 (2000)
34. Chen, Y., Ding, Y.: Posture optimization in robotic flat-end milling based on sequential quadratic programming. *J. Manuf. Sci. Eng.* **145**, 061001 (2023)
35. Usevitch, N.S., Hammond, Z.M., Schwager, M.: Locomotion of linear actuator robots through kinematic planning and nonlinear optimization. *IEEE Trans. Rob.* **36**, 1404–1421 (2020)
36. Gaz, C., Cognetti, M., Oliva, A., Robuffo Giordano, P., De Luca, A.: Dynamic identification of the franka emika panda robot with retrieval of feasible parameters using penalty-based optimization. *IEEE Robotics Automation Lett.* **4**, 4147–4154 (2019)
37. Todorov, E., Erez, T., Tassa, Y.: Mujoco: A physics engine for model-based control. 2012 IEEE/RSJ Int. Conf. on Intelligent Robots and Systems (2012)
38. Kato, Y., et al.: A self-tuning impedance-based interaction planner for robotic haptic exploration. *IEEE Robotics Automation Lett.* **7**, 9461–9468 (2022)
39. Peternel, L., Petrič, T., Babič, J.: Robotic assembly solution by human-in-the-loop teaching method based on real-time stiffness modulation. *Auton. Robot.* **42**, 1–17 (2018)

**Publisher's Note** Springer Nature remains neutral with regard to jurisdictional claims in published maps and institutional affiliations.

Springer Nature or its licensor (e.g. a society or other partner) holds exclusive rights to this article under a publishing agreement with the author(s) or other rightsholder(s); author self-archiving of the accepted manuscript version of this article is solely governed by the terms of such publishing agreement and applicable law.

**Nikola Knežević** graduated in 2016 and completed his Master's studies in 2018 at the Faculty of Electrical Engineering, University of Belgrade (ETF). He enrolled in his Ph.D. studies at the Faculty of Electrical Engineering in 2018. Nikola has been employed at the Faculty of Electrical Engineering, University of Belgrade as a teaching assistant since 2019. He is engaged in the control of robotic systems with compliant joints and physical human-robot interaction. Also, the focus of his research is learning techniques that can be used in robotics systems.

**Branko Lukić** is a Research Associate at the University of Belgrade - School of Electrical Engineering (ETF) and a member of the ETF Robotics lab. He gained his PhD degree in Robotics in 2022 at ETF. He conducted part of his PhD research in the Laboratory for the Advancement of Collaborative Robot Behavior in Physical Human-Robot Interaction (CoBoTaT) at the Jožef Stefan Institute in Slovenia. His research interests are modelling and control of compliant actuators, human-robot interaction control, and modelling and control of compliant robots. He was a participant in several national and bilateral research projects.

**Tadej Petrič** is a senior research associate in the Department of Automation, Biocybernetics and Robotics at the Jožef Stefan Institute and an assistant professor at the Jožef Stefan International Postgraduate School, Slovenia. He is also the head of the Laboratory for the Advancement of Collaborative Robot Behaviour in Physical Human-Robot Interaction (CoBoTaT). In 2015, he was a postdoctoral fellow at Biorob (Prof. Auke Ijspeert lab) at École polytechnique fédérale de Lausanne (EPFL). In 2013, he received a PhD in Robotics from the Faculty of Electrical Engineering, University of Ljubljana. He conducted part of his PhD research in the Department of Robotic Systems for Dynamic Control of Legged Humanoid Robots at the German Aerospace Center (DLR) in Germany. In 2013, he was a visiting researcher at ATR Computational Neuroscience Laboratories in Japan. His current research focuses on the design of biologically plausible robotic controllers that achieve robustness and adaptation to changing environments comparable to humans.

**Kosta Jovanović** is an Associate Professor at the University of Belgrade - School of Electrical Engineering (ETF) and Head of ETF Robotics lab ([www.robot.etf.rs](http://www.robot.etf.rs)). He gained his Ph.D. degree in Robotics at University of Belgrade in 2016. He gained professional experience in German Aerospace Center (DLR), Technical University of Munich, and company SMS Siemag, all in Germany. His research interests are modeling and control of collaborative robots, mechanical impedance estimation and physical human-robot collaboration in medical and industrial applications. He has been the principal investigator on behalf of ETF in several European and national projects in robotics, including project CircuBot funded by the Science Fund of the Republic of Serbia under the Green Program of Cooperation between Science and Industry.